

# Water Injectivity Tests on Multilayer Reservoir: Approximate Solution for Pressure Behavior during a Multiple Flow-rate Scheme

Jessica L. F. Bittencourt Neto<sup>a,\*</sup>, Sinesio Pesco<sup>a</sup>, Abelardo Borges Barreto Jr.<sup>a</sup>

<sup>a</sup>*PUC-Rio, Departamento de Matemática*

---

## Abstract

An injectivity test consists of continuously injecting a phase (water or gas), for a period of time, into an oil-saturated reservoir. From the analysis of the wellbore pressure behavior, this procedure aims to estimate, in addition to the volume of recoverable oil, reservoir parameters, such as permeability, skin effect among others. In this context, this work aims to propose an approximate analytical solution for the pressure behavior during a water injectivity test on a multilayer reservoir considering a scheme of multiple injection flow-rates. The accuracy of the proposed solution was evaluated by comparison to a commercial finite difference-based flow simulator in different scenarios. Results express a considerable agreement between the data provided by the numerical simulator and the proposed model. In addition, from the proposed model it was possible to estimate the reservoir equivalent permeability with satisfactory results.

**Keywords:** Injectivity Test, Multilayer Reservoir, Multiple Flow-Rate, Permeability Estimation

---

## 1. Introduction and Background

Injectivity test is a method based on injecting a fluid into a reservoir (usually, water) to optimize oil extraction or obtain information about the reservoir. From the pressure response received in this process, relevant information regarding the reservoir can be obtained, such as equivalent permeability, recoverable oil volume, among others.

Considering a single-phase flow, in 1987, Ehlig-Economides et al. [1] propose a new method to estimate each reservoir layer's properties and interpret them. Such methods are based on the analysis of pressure and flow-rate for each layer. Thus, it is possible to determine the permeability and formation damage of each layer. In reservoirs with cross-flow formations, the vertical permeability between the layers could also be estimated

In 1989, Raghavan [2] synthesized the advances until then regarding multilayer reservoirs under single-phase flow. His main objective was to extend the available pressure analysis methods of

---

\*I am corresponding author

Email addresses: [jessica.fbn@puc-rio.br](mailto:jessica.fbn@puc-rio.br) (Jessica L. F. Bittencourt Neto), [sinesio@puc-rio.br](mailto:sinesio@puc-rio.br) (Sinesio Pesco), [abelardo.puc@gmail.com](mailto:abelardo.puc@gmail.com) (Abelardo Borges Barreto Jr.)

commingled fluid production, examining the characteristics of standard semilog techniques.

Thompson and Reynolds [3] present in 1997 a pressure-transient behavior study of single and multiphase flow in radially heterogeneous reservoirs the light of a mobility averaging theory that is based on Darcy's law. Therefore, the model can apply to injectivity tests.

In 2001, Peres and Reynolds [4] propose an approximated analytical solution for injectivity tests on horizontal wells. The results are compared with a numerical simulator. Then, it is shown that the approximated solution is sufficiently accurate for practical applications. Besides that, it is shown that one can easily construct dimensionless solutions without resorting to numerical simulation.

Approximate analytical solutions for the injection pressure response at a horizontal water injection well have been presented by Peres et al. [5] in 2004.

Subsequently, Peres et al. [6] used the superposition principle to provide a solution during the falloff period. Although the injection problem is not linear, the authors followed Abbaszadeh and Kamal [7] and Bratvold and Horne [8] works. They demonstrated that the analytical solution for the falloff period could be obtained with reasonable precision under the assumption that the total mobility profile remains stationary after the well is shut-in and using an expression for the flow-rate profile obtained.

Barreto et al. [9] in 2011 propose an analytical solution for vertical water injector well completed in a multilayer commingled reservoir. This solution is used to compute the wellbore pressure, injection flow-rates, and the waterfront for each layer.

Also, parameter estimation can be obtained from the proposed solution.

In 2019, Bela et al. [10] propose an analytical solution to the falloff period in multilayered reservoirs based on the use of a dimensionless flow-rate. The model efficiency was verified by comparison to a numerical simulator.

Finally, in 2020 Bonafé et al. [11] presented a new formulation to approximate the pressure response at the well when performing injectivity tests with multiple flow-rates in a single layer reservoir. The proposed formulation is also used to determine the reservoir permeability of any specific injection or falloff period. The accuracy of the proposed solution was also assessed by comparison to a numerical simulator.

This paper proposes an approximate solution for the pressure response in a multilayer reservoir with a vertical well during an injectivity test with multiple flow-rate schemes. The proposed formulation was reached by extending and generalizing the existing injection-falloff solutions presented by [9], [10], and [11], considering the total volume of injected water into the reservoir during the test. The proposed solution's accuracy was evaluated by comparison to a commercial flow simulator, considering a selected set of synthetic cases. The model will also be used to compute parameters related to both water and oil phases for each injection period.

## 2. Mathematical Model

Starting from the formulation for an injectivity test in a single layer reservoir with constant flow proposed by Peres et. al [5], Bonafé [11] proposed a formulation

for an injectivity test in a single layer reservoir using a multiple flow-rate scheme. Following these works, this paper will develop the formulation that describes the pressure behavior during water injection in a multilayer reservoir considering a multiple flow-rate scheme. In this formulation, a reservoir with  $n$ -layers will be considered. Water injection occurs with a multiple flow scheme considering  $m$ -injection periods. The Figure 1 shows an example of this reservoir model.

For the mathematical formulation, the following hypotheses are assumed:

- Reservoir is homogeneous and isotropic, with infinite extension;
- Negligible gravitational and capillary forces;
- Water and oil are considered immiscible and slightly compressible fluids with constant viscosity ( $\mu$ );
- Isothermal flow;
- Constant thickness in each layer ( $h_j$ );
- The well fully penetrates all layers;
- The well injects a constant flow rate  $q_i$  at each injection period  $i$ ;
- The rock formation has a small and constant compressibility;
- There is no wellbore storage effect;
- There is no damaged region close to the well (skin);
- At time  $t = 0$ , the reservoir is in equilibrium, that is, the pressure is the same in all layers.

Therefore, the flow-rate behavior in the well is described according to the following scheme:

$$q_{inj}(t) = \begin{cases} q_0 = 0, & t_0 = 0 \\ q_1 = \sum_{j=1}^n q_{j1}, & t_0 < t \leq t_1 \\ q_2 = \sum_{j=1}^n q_{j2}, & t_1 < t \leq t_2 \\ \vdots & \vdots \\ q_m = \sum_{j=1}^n q_{jm}, & t_{m-1} < t \leq t_m \end{cases} \quad (1)$$

where  $q_{ji}$  represents the injection flow-rate in layer  $j$  at the injection period  $i$ , while  $q_i$  represents the injection flow-rate in the well in the injection period  $i$ .

### 3. Formulation for Multilayer Reservoirs

This section synthetize the solution of the pressure behavior on a multilayer reservoir during water injectivity test found in previous works. The fluid mobility ( $\lambda_f$ ) measures the easiness of a fluid to flow through the porous medium. So, following the work [3], this property is defined as the ratio between the relative permeability of the phase and its viscosity, that is:

$$\lambda_f(S_w) = \frac{k_{rf}(S_w)}{\mu_f} \quad (2)$$

where,  $f = w, o$ .

Thus, the total mobility of the oil-water system can be defined as:

$$\lambda_t(S_w) = \lambda_o(S_w) + \lambda_w(S_w) \quad (3)$$

Using Darcy's law, oil and water flow-rates are given by:

$$q_{oj}(r, t) = -2\pi h_j k_j \lambda_{oj} \left( r \frac{\partial p_j(r, t)}{\partial r} \right) \quad (4)$$

and

$$q_{wj}(r, t) = -2\pi h_j k_j \lambda_{wj} \left( r \frac{\partial p_j(r, t)}{\partial r} \right) \quad (5)$$

By mass conservation, total flow in layer  $j$  is obtained by:

$$q_j(r, t) = q_{o_j}(r, t) + q_{w_j}(r, t) \quad (6)$$

Thereby, replacing equations (4) and (5) in Equation (6):

$$q_j(r, t) = -2\pi h_j k_j (\lambda_{o_j} + \lambda_{w_j}) \left( r \frac{\partial p_j(r, t)}{\partial r} \right) \quad (7)$$

During an injection period a water saturation region is formed around the well. Over time, this region propagates, so saturation is a function of time and radius. Therefore, Equation (7) can be rewritten as follows:

$$q_j(r, t) = -2\pi h_j k_j \lambda_{t_j}(r, t) \left( r \frac{\partial p_j(r, t)}{\partial r} \right) \quad (8)$$

Rearranging the terms of the Equation (8):

$$\frac{\partial p_j(r, t)}{\partial r} = -\frac{1}{2\pi h_j k_j} \frac{q_j(r, t)}{\lambda_{t_j}(r, t) r} \quad (9)$$

From the assumptions the reservoir is infinite. Therefore, integrating both sides of Equation (9) from the well:

$$\Delta p_{wf_j} = \frac{1}{2\pi h_j k_j} \int_{r_w}^{\infty} \frac{q_j(r, t)}{\lambda_{t_j}(r, t) r} dr \quad (10)$$

On the other hand, the water injected volume ( $v_{ji}$ ) at layer  $j$ , for  $t_{i-1} \leq t \leq t_i$ , where  $i = 1, \dots, m$ , can be defined as:

$$v_{ji}(t) = \int_0^t q_{ji}(t') dt' \quad (11)$$

Thus, considering the Buckley-Leveret formulation [12], the waterfront radius ( $r_{F_j}$ ) can be defined as:

$$r_{F_j}(t) = \sqrt{r_w^2 + \frac{v_{ji}(t) B_w}{24\pi h_j \phi} f'_{w_j}(S_w)} \quad (12)$$

It is important to note that  $f'_{w_j}(S_w)$  represents the water fractional flow derivative in layer  $j$ , at each saturation point ( $S_w$ ). The fractional flow curve depends on the mobility of the fluid:

$$f_{w_j}(S_w) = \frac{\lambda_{w_j}(S_w)}{\lambda_{t_j}(S_w)} \quad (13)$$

In each layer, it is easy to notice that in the region where  $r > r_{F_j}$  only oil flows. Thus, using the constants of adequacy to the system of measures  $\alpha_p$ , the integral of Equation (9) can be reformulated as the following sum:

$$\Delta p_{wf_j} = \frac{\alpha_p}{h_j k_j} \int_{r_w}^{r_{F_j}(t)} \frac{q_j(r, t)}{\lambda_{t_j}(r, t) r} dr + \frac{\alpha_p}{h_j k_j} \int_{r_{F_j}(t)}^{\infty} \frac{q_{o_j}(r, t)}{\hat{\lambda}_{o_j} r} dr \quad (14)$$

where  $\alpha_p = 19.03$ .

Adding and subtracting the term  $\frac{\alpha_p}{h_j k_j} \int_{r_w}^{r_{F_j}(t)} \frac{q_{o_j}(r, t)}{\hat{\lambda}_{o_j} r} dr$  on the right side of the Equation (14):

$$\Delta p_{wf_j} = \frac{\alpha_p}{h_j k_j} \int_{r_w}^{r_{F_j}(t)} \left( \frac{q_j(r, t)}{\lambda_{t_j}(r, t)} - \frac{q_{o_j}(r, t)}{\hat{\lambda}_{o_j}} \right) \frac{dr}{r} + \frac{\alpha_p}{h_j k_j} \int_{r_w}^{\infty} \frac{q_{o_j}(r, t)}{\hat{\lambda}_{o_j} r} dr \quad (15)$$

Equation (15) shows that the pressure variation in the well can be understood as the sum of two terms: one due to differences in mobility between oil and water ( $\Delta p_{\lambda_j}$ ) and another related to the single-phase oil flow ( $\Delta p_{o_j}$ ):

$$\Delta p_{wf_j}(t) = \Delta p_{\lambda_j}(t) + \Delta p_{o_j}(t) \quad (16)$$

where:

$$\Delta p_{\lambda_j}(t) = \frac{\alpha_p}{h_j k_j} \int_{r_w}^{r_{F_j}(t)} \left( \frac{q_j(r, t)}{\lambda_{t_j}(r, t)} - \frac{q_{o_j}(r, t)}{\hat{\lambda}_{o_j}} \right) \frac{dr}{r} \quad (17)$$

and

$$\Delta p_{o_j}(t) = \frac{\alpha_p}{h_j k_j} \int_{r_w}^{\infty} \frac{q_{o_j}(r, t)}{\hat{\lambda}_{o_j}} \frac{dr}{r} \quad (18)$$

The approximated solution of Equation (16) was presented by [9].

#### 4. Proposed Formulation

To determine the pressure variation along the reservoir, an approximation for the multiple flow-rate scheme in each layer ( $\bar{q}_j$ ) will be used. Assuming that the flow through each layer can be approximated by the flow in the flooded region or by the oil flow ahead of the flooded region:

$$\bar{q}_j(r, t) \approx q_j(r, t) \approx q_{o_j}(r, t) \quad (19)$$

Therefore, the term referring to the mobility difference between water and oil in layer  $j$ , explained at the previous section by Equation (14), can be rewritten as follows:

$$\Delta p_{\lambda_j}(t) = \frac{\alpha_p}{h_j k_j \hat{\lambda}_{o_j}} \int_{r_w}^{r_{F_j}(t)} \bar{q}_j(r, t) \left( \frac{\hat{\lambda}_{o_j}}{\hat{\lambda}_{t_j}(r, t)} - 1 \right) \frac{dr}{r} \quad (20)$$

By hypothesis, pressure variation at the well in each layer is the same, that is:

$$\Delta p_{wf}(t) = \Delta p_{wf_1}(t) = \dots = \Delta p_{wf_n}(t) \quad (21)$$

As an algebraic device, the pressure variations in the well in each layer can be added. This mathematical device, despite having no physical sense, helps to obtain a general solution for pressure variation at the well.

From this, using Equations (16) and (21), two equalities are obtained:

$$\begin{aligned} \sum_{j=1}^n \Delta p_{wf_j}(t) &= n \Delta p_{wf}(t) = \\ &= \sum_{j=1}^n (\Delta p_{\lambda_j}(t) + \Delta p_{o_j}(t)) \end{aligned} \quad (22)$$

So:

$$\Delta p_{wf}(t) = \frac{1}{n} \left( \sum_{j=1}^n \Delta p_{\lambda_j}(t) + \sum_{j=1}^n \Delta p_{o_j}(t) \right) \quad (23)$$

On the other hand, the single-phase solution ensures that  $\Delta p_{o_j}$  is in fact the same in all layers [9]. That is:

$$\Delta p_o(t) = \Delta p_{o_1}(t) = \dots = \Delta p_{o_n}(t) \quad (24)$$

Thus,

$$\sum_{j=1}^n \Delta p_{o_j} = n \Delta p_o(t) \quad (25)$$

Where  $\Delta p_o(t)$  is the pressure change obtained from the solution for single-phase flow problem given by:

$$\Delta p_o = \frac{\alpha_p B \mu_o}{k_{eq} h_i} \sum_{k=1}^i \left[ (q_k - q_{k-1}) \left( -\frac{1}{2} E_i \left( \frac{-r_w^2 \phi \mu_o c_t}{4 \alpha_t k_{eq} (t - t_{k-1})} \right) \right) \right] \quad (26)$$

Finally, replacing Equation (25) in Equation (23) it is possible to obtain an approximate expression for the pressure behavior in the well:

$$\Delta p_{wf}(t) = \frac{1}{n} \sum_{j=1}^n \Delta p_{\lambda_j}(t) + \Delta p_o(t) \quad (27)$$

It is important to note that for a single layer problem the solution proposed in the Equation (27) reduces to the solution proposed by Bonafé et al [11].

## 5. Flow-rate scheme approach

In the formulation proposed in Section 4 a crucial step is relative to use an approach for the flow-rate at each reservoir layer. To determine this approach a same reasoning proposed by [11] was followed.

For a single-layer reservoir and considering a single-phase flow with constant flow-rate, from the combination of the mass conservation equation, Darcy's law and state equations, the solution for the pressure is given by:

$$\Delta p(r, t) = \frac{\alpha_p q B}{h k \hat{\lambda}_o} \left[ -\frac{1}{2} E_i \left( -\frac{r^2 \phi \hat{c}_t}{4 \alpha_t k \hat{\lambda}_o t} \right) \right] \quad (28)$$

Thus, for a single-phase flow and considering a single-layer reservoir with a multiple flow-rate scheme, it is possible to apply flow-rate superposition. Therefore, the pressure solution is now given by:

$$\Delta p(r, t) = \frac{1}{2} \frac{\alpha_p B}{h k \hat{\lambda}_o} \sum_{k=1}^i (q_k - q_{k-1}) \left[ E_i \left( -\frac{r^2 \phi \hat{c}_t}{4 \alpha_t k \hat{\lambda}_o (t - t_k)} \right) \right] \quad (29)$$

On the other hand, by Darcy's law:

$$q(r, t) = \frac{h k \hat{\lambda}_o}{\alpha_p B} \left( r \frac{\partial p(r, t)}{\partial r} \right) \quad (30)$$

So, replacing the Equation (29) in (30):

$$q(r, t) = \sum_{k=1}^i \left[ (q_k - q_{k-1}) e^{-\frac{r^2 \phi \hat{c}_t}{4 \alpha_t k \hat{\lambda}_o (t - t_{k-1})}} \right] \quad (31)$$

Therefore, in the formulation proposed in Section 4, for a multilayer reservoir the flow-rate in layer  $j$  in a given injection period  $i$  can be approximated by profile flow-rate obtained for a single phase flow:

$$q_j(r, t) = \sum_{k=1}^i \left[ (q_{jk} - q_{jk-1}) e^{-\frac{r^2 \phi \hat{c}_t}{4 \alpha_t k_j \hat{\lambda}_{oj} (t - t_{k-1})}} \right] \quad (32)$$

## 6. Results and Discussion

The accuracy of the proposed solution was evaluated by comparison with a commercial flow simulator based on finite differences. Scenarios considering different reservoir properties were used in such comparisons. To correctly interpret the results of an injectivity test, it is necessary to analyze the pressure data and the pressure derivative curve concerning the natural logarithm of time. For numerical calculations, the pressure derivative was calculated as proposed by Bourdet [13] for each time variation, and for numerical integration, the trapezoidal rule was used.

### 6.1. Comparison with the Numerical Simulator

For all cases of this section, a total injection period of 72 hours (3 days) was considered, where each period refers to 24 hours (1 day) of injection, according to Table 1. In each case group, scenarios with different permeability in each layer and different oil viscosity values were considered. The relative permeability curves showed in Figure 2 are evaluated for each layer.

Cases A and B were divided into four cases, according to Table 2. In these cases, two pairs of cases with different reservoir properties were considered. The difference between these sub-cases is the oil viscosity used, which influences the oil mobility value ( $\lambda_o$ ). The mobility ratio is a useful variable to interpret which fluid moves more easily in the porous medium. This parameter has no physical meaning and comes from the mobility ratio curve M, which expresses the ratio between two corresponding points on the mobility curves:

$$M(S_w) = \frac{\lambda_w(S_w)}{\lambda_o(S_w)} \quad (33)$$

Thus, the mobility ratio ( $\hat{M}$ ) will be defined as the ratio between the water mobility in the

residual oil saturation and the oil mobility in the initial water saturation:

$$\hat{M} = \frac{\lambda_w(S_{or})}{\lambda_o(S_{wi})} = \frac{\hat{\lambda}_w}{\hat{\lambda}_o} \quad (34)$$

Because of that, in cases where  $\hat{M} > 1$ , the flow is favorable to water, while in cases where  $\hat{M} < 1$  flow is unfavorable to water. The graphs presented in this section are on the log-log scale to facilitate the visualization of the transient pressure pulse. The presented results were divided into two groups of cases according to the injection flow-rates schemes.

**Cases A:** In this set of cases, the injection rate increases gradually at each period. The first two cases to be presented, called Cases A1 and A2, have the same characteristics shown in Table 2. For case A1, it is possible to observe good agreement between the curves in all periods shown in Figure 3. Figure 4 show the results for case A2, it is possible to observe a small discrepancy between the derivative curves at a given time. This occurs because of the spatial discretization of the flow simulator and due to shocks in the solution inherent to the problem. Thus, the response of the flow simulator is felt later in comparison to the analytical response.

**Cases B:** In this set of cases, reservoir properties are the same as those used in case A, but the flow-rate scheme is different. As shown in Table 2, injection flow-rates are gradually reduced during injection periods. Consequently, the pressure curves for the 2nd and 3rd periods are decreasing. In general, although the injection flow rates in Cases B are different from those in Cases A, the behaviors and the causes of the curves' errors are similar. It is also possible to observe a good similarity between the curves in Figures 5 and 6 for Cases B1 and B2, respectively.

In general, the graphs showed a good correspondence between the curves of the derivatives of the model built in this work and the curves generated by the flow simulator.

Thus, it is possible to conclude that the model presented for the problem is useful. The formulation presented can be used for modeling a large number of flow-rates or reservoir layers.

## 6.2. Estimated Equivalent Permeability

The proposed solution can also be applied to estimate the reservoir equivalent permeability. To evaluate the accuracy of the estimated permeability, two long-term injectivity tests with 516 hours-flow were considered. The cases in this section are called C and D and use the multiple flow-rate scheme in Table 3. Besides that, the reservoir properties used as input parameters can be seen in the Table 4.

The reservoir equivalent permeability is calculated using the permeabilities of each layer inserted in the simulation. Thus, the reservoir equivalent permeability is given by the following expression:

$$k_{eq} = \frac{k_1 h_1 + \dots + k_n h_n}{h_t} \quad (35)$$

On the other hand, for the single-phase flow case with constant flow-rate, it is known that the pressure change at the wellbore is given by:

$$\Delta p_o(t) = 1.151 \frac{\alpha_p q B}{h k \hat{\lambda}_o} \log \left( \frac{4 \alpha_t k \hat{\lambda}_o t}{e^{\gamma} c_t \phi r_w^2} \right) \quad (36)$$

It is easy to notice that Equation (36) represents a linear graph against the natural logarithm of time whose inclination is given by:

$$m_o = 1.151 \frac{\alpha_p q B}{h k \hat{\lambda}_o} \quad (37)$$

The line slope allows estimating the reservoir equivalent permeability for single-phase flow.

Adapting this interpretation to a multiple flow-rate scheme, the change of injection flow-rate ( $\Delta q_i$ ) will be used. This is defined as the absolute value of the injection flow difference of two subsequent periods:

$$\Delta q_i = |q_i - q_{i-1}| \quad (38)$$

Graphs of pressure data normalized by the change of the injection flow-rate help to identify the similarity between the pressure derivative levels. Such levels, can be associated through an interpretation method with the oil or water properties in Figures 7, 8, 9, 10.

Similarly to the interpretation for single phase flow, it is possible to estimate the reservoir equivalent permeability. Analyzing the pressure logarithmic derivative curve at each injection period, the properties of each fluid are used. Figures 7, 8, 9, 10 show the normalized pressure and derivative pressure curves for all periods.

It is important to note that pressure behavior in the well is similar to the single-phase oil flow during the first injection period since the region close to the well is saturated with oil. However, in subsequent periods, this region is now saturated with water. Thus, the well bottom-hole pressure behavior becomes similar to the single-phase water flow.

Therefore, in general, for two-phase flow, two slopes corresponding to the oil and water mobilities must be considered, depending on the injection period. Because of that, for cases C1, C2, D1, and D2, Figures 11, 12, 13 and 14, respectively, show the slopes correspondent to water and oil properties from the derivative curve. With these values, it is possible to calculate the estimated reservoir permeability using the relative permeability (water and oil) endpoints.

$$\bar{k}_{eq_o} = 1.151 \frac{\alpha_p \Delta q B_w}{h_t \hat{\lambda}_o m_o} \quad (39)$$

and

$$\bar{k}_{eq_w} = 1.151 \frac{\alpha_p \Delta q B_w}{h_t \hat{\lambda}_w m_w} \quad (40)$$

Thus, the results obtained in cases C1, C2, D1 and D2 for the calculated equivalent permeability and the percentage error compared to the reservoir equivalent permeability can be seen in Tables 5, 6, 7 and 8, respectively.

The results obtained for estimated reservoir permeability compared to reference permeability, in general, are very close for all periods. These results prove the effectiveness of the proposed model to estimate the reservoir equivalent permeability.

## 7. Conclusions

Based on the formulation for the falloff period by [10] in multilayer reservoirs, and the formulation for injectivity tests with multiple flow-rates by [11], it was possible to propose a solution for the pressure behavior on multilayer reservoirs considering multiple flow-rate schemes in this work. The developed analytical model can also be used as a basis for future work. As an example, the presented solution can be extended to a solution in the Laplace Domain for multilayer reservoirs and multiple flow-rate schemes. Moreover, the model presented can also be used as a basis for similar formulations considering a damage region (skin) or temperature effects. The proposed model was applied in a set of cases with different reservoir properties, such as a different number of layers, permeabilities, and injection flow-rates. The comparison between the approximate analytical solution and the numerical simulator indicated good agreement for all tested cases. Furthermore, it was also possible to estimate the reservoir equivalent permeability during each injection period. The low error obtained for the estimated equivalent permeability proves that the proposed model effectively estimates this reservoir parameter.

## Nomenclature

- $c_t$  = Total compressibility
- $f_w$  = Fractionary flow
- $f'_w$  = Fractionary flow derivative
- $h_j(m)$  = Thickness of layer  $j$
- $h_t(m)$  = Reservoir total thickness
- $k_{eq}(mD)$  = Reservoir equivalent permeability
- $k_j(mD)$  = Permeability in layer  $j$

$\hat{M}$  = Endpoint mobility ratio  
 $p_{wf}(kgf/cm^2)$  = Wellbottom hole pressure  
 $q_{inj}(m^3/day)$  = Injection flow-rate  
 $q_j((m^3/day))$  = Injection flow-rate in each layer  $j$   
 $r_{Fj}(m)$  = Waterfront radius in layer  $j$   
 $r_w(m)$  = Wellbore radius  
 $S_w$  = Water saturation  
 $t(h)$  = Time  
 $\alpha_p$  = Pressure unit conversion constant  
 $\alpha_t$  = Time unit conversion constant  
 $\gamma$  = Euler constant  
 $\lambda_o$  = Endpoint oil mobility  
 $\hat{\lambda}_w$  = Endpoint water mobility  
 $\lambda_t$  = Total mobility  
 $\phi$  = Porosity  
 $\mu_o(cP)$  = Oil Viscosity  
 $\mu_w(cP)$  = Water Viscosity

## Acknowledgements

The authors are grateful to Petrobras and CAPES for the financial support during this work. The authors also would like to thanks the PhD Student Renan Vieira Bela, from Math Department of PUC-Rio, for review support.

## References

- [1] EHLIG-ECONOMIDES, C. A.; JOSEPH, J., A New Test for Determination of Individual Properties in a Multilayered Reservoir, SPE Formation Evaluation. (1987) 261–283.
- [2] RAGHAVAN, R., Behavior of Wells Completed in Multiple Producing Zones, SPE Formation Evaluation (1989) 219–230.
- [3] THOMPSON, L. G.; REYNOLDS, A. C., Well Testing for Radially Heterogeneous Reservoirs Under Single and Multiphase Flow Conditions, SPE Formation Evaluation (1997) 57–64.
- [4] PERES, A. M. M.; REYNOLDS, A. C., Theory and Analysis of Injectivity Tests on Horizontal Wells, SPE Journal June (2003) 147–159.
- [5] PERES, A. M. M.; BOUGHARA, A. A.; CHEN, S.; MACHADO, A. A. V.; REYNOLDS, A. C., Approximate Analytical Solutions for the Pressure Response at a Water Injection Well, Paper presented at the Annual Technical Conference and Exhibition September (2004) 1–17.
- [6] PERES, A. M. M.; BOUGHARA, A. A.; REYNOLDS, A. C., Rate Superposition for Generating Pressure Falloff Solutions, SPE Journal September (2004) 364–374.
- [7] ABBASZADEH, M.; KAMAL, M., Pressure-Transient Testing of Water-Injection Wells, SPE Reservoir Engineering. (1989) 115–124.
- [8] BRATVOLD, R. B.; HORNE, R. N., Analysis of Pressure-Falloff Tests Following Cold-Water Injection, SPE Formation Evaluation (1990) 293–302.
- [9] BARRETO JR, A.; PERES, A.; PIRES, Water Injectivity Tests on Multilayered Oil Reservoirs, Brasil Offshore Conference and Exhibition (2011) 1–11.
- [10] BELA, R. V.; PESCO, S.; BARRETO, A. B., Modeling Falloff Tests in Multilayer Reservoirs, Journal of Petroleum Science and Engineering (2019) p.
- [11] BONAFÉ, M. F.; BRAGA, A.; BARRETO, A. B., Approximate Solution for Pressure Behavior during a Multiple Rate Injectivity Test, submitted to Journal of Petroleum Exploration and Production Technology (2020) 1–14.
- [12] BUCKLEY, S. E.; LEVERETT, M. C., Mechanism of Fluid Displacement in Sands, Petroleum Technology May (1941) 107–116.
- [13] BOURDET, D.; AYOUB, J. A.; PLRARD, Y. M., Use of Pressure Derivative in Well-Test Interpretation, SPE Formation Evaluation. June (1989) 293–302.

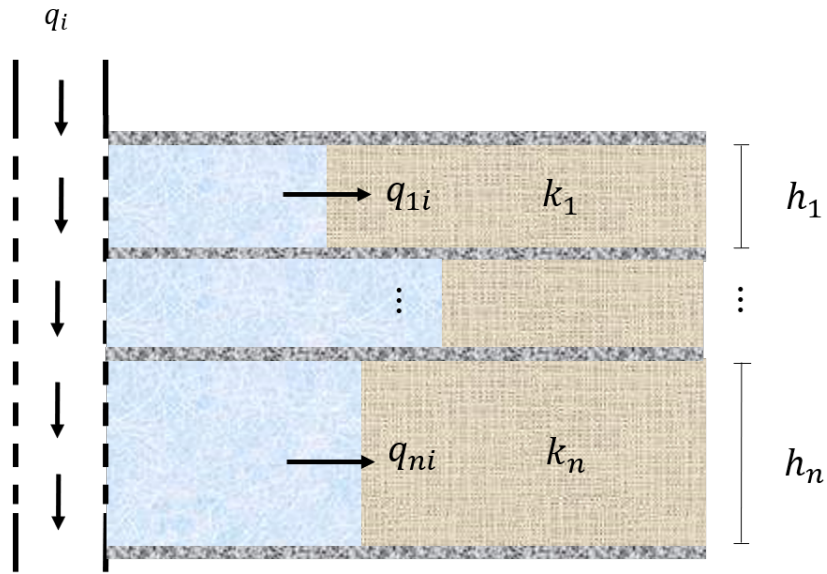


Figure 1: Reservoir model with  $n$  layers and two-phase flow

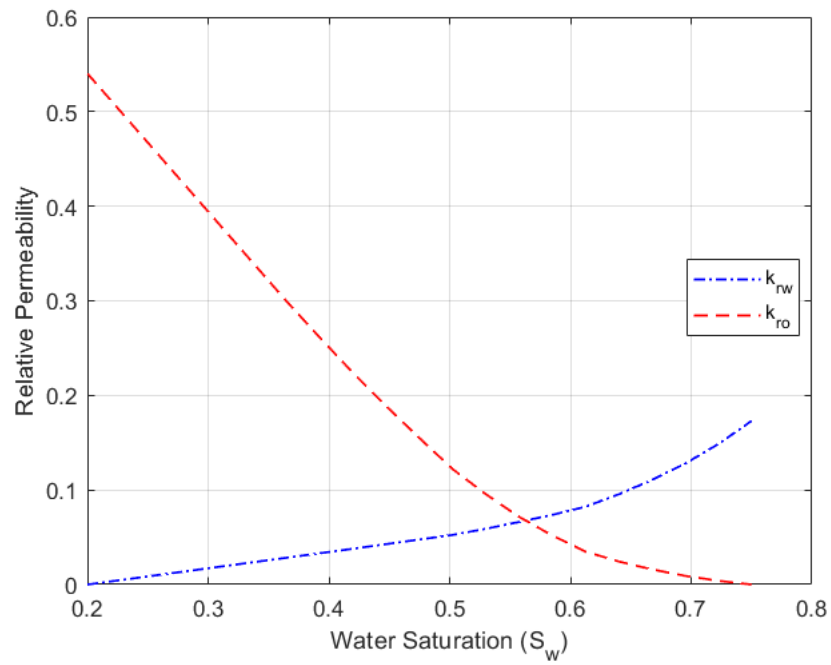


Figure 2: Relative permeability curves

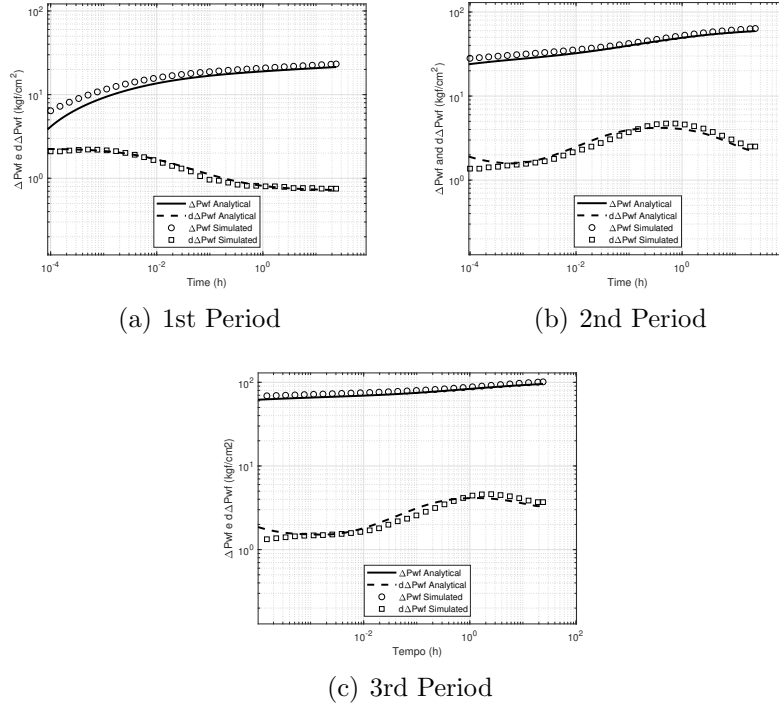


Figure 3: Pressure and pressure derivative curves for case for case A1

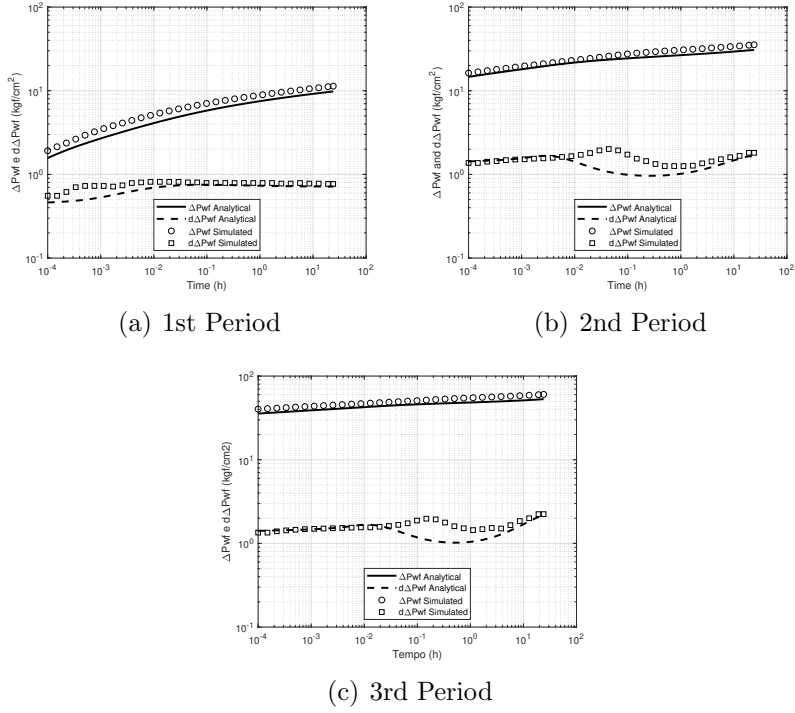


Figure 4: Pressure and pressure derivative curves for case A2

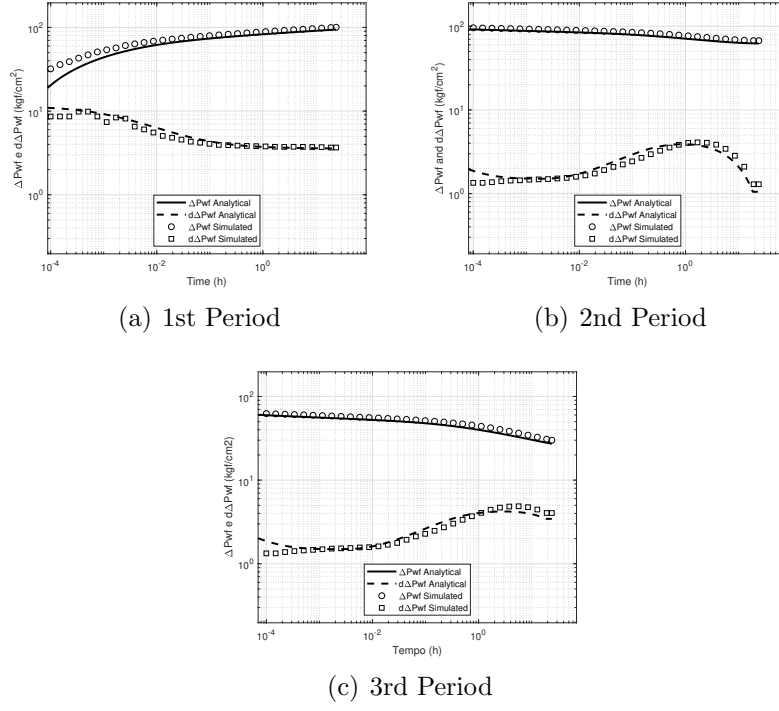


Figure 5: Pressure and pressure derivative curves for case B1

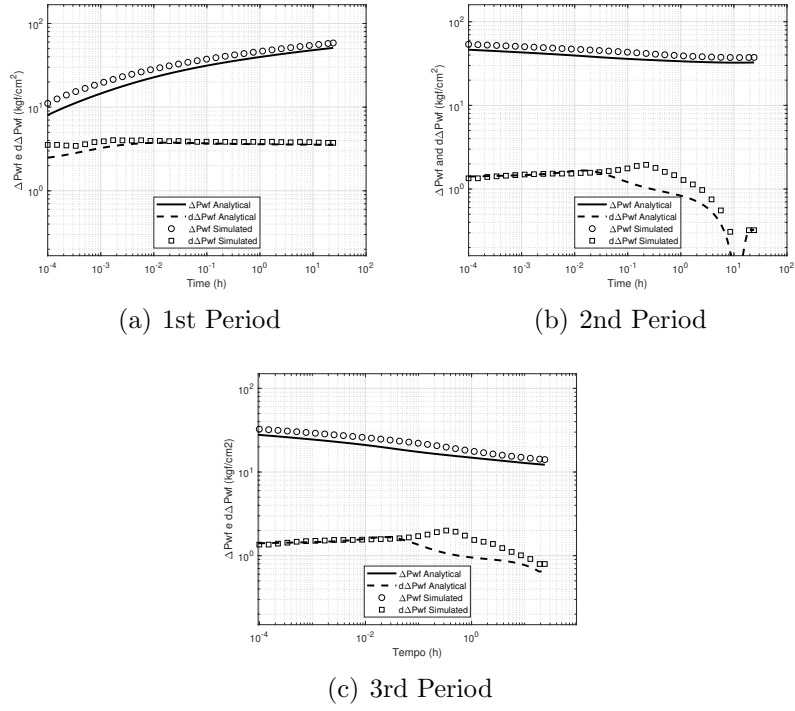
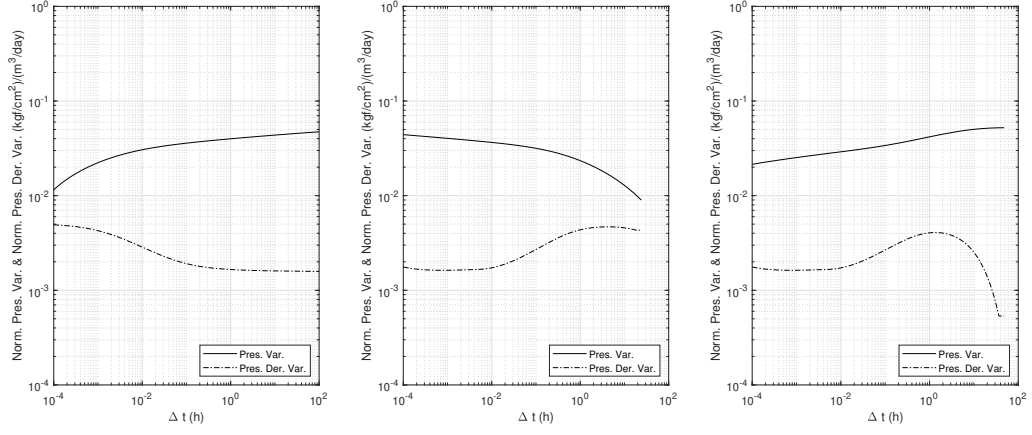
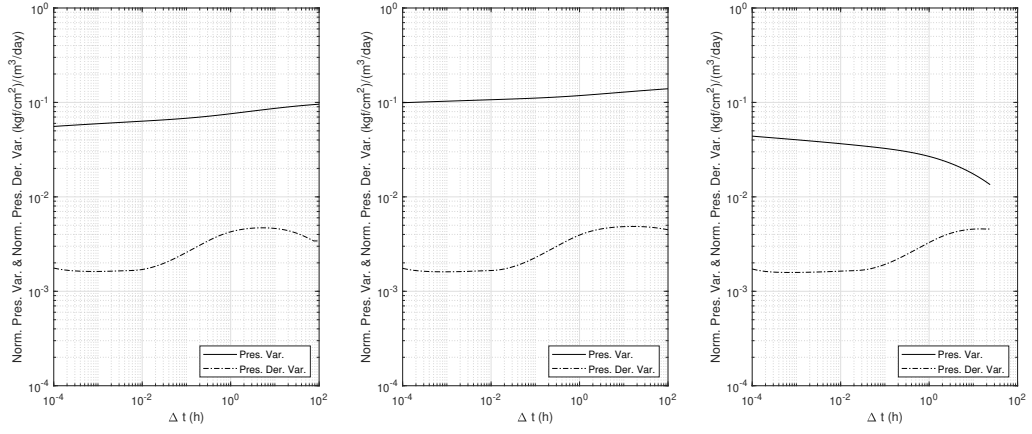


Figure 6: Pressure and pressure derivative curves for case B2



(a) 1st, 2nd and 3rd injection period

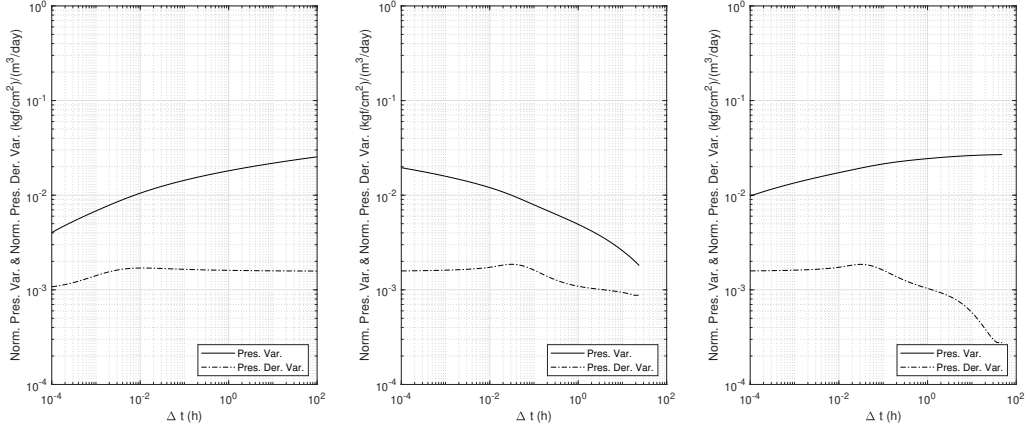


(b) 4th, 5th and 6th injection period

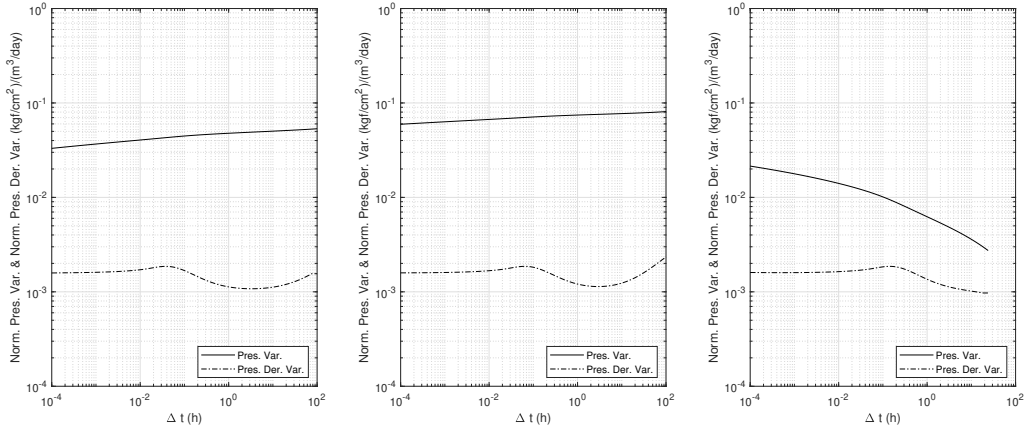
Figure 7: Normalized pressure and pressure derivative curves for case C1

Cases	Injection Period	Flow-rate scheme ( $m^3/day$ )
A	1	500
	2	1500
	3	2500
B	1	2500
	2	1500
	3	500

Table 1: Flow-rate schemes for cases A and B



(a) 1st, 2nd and 3rd injection period

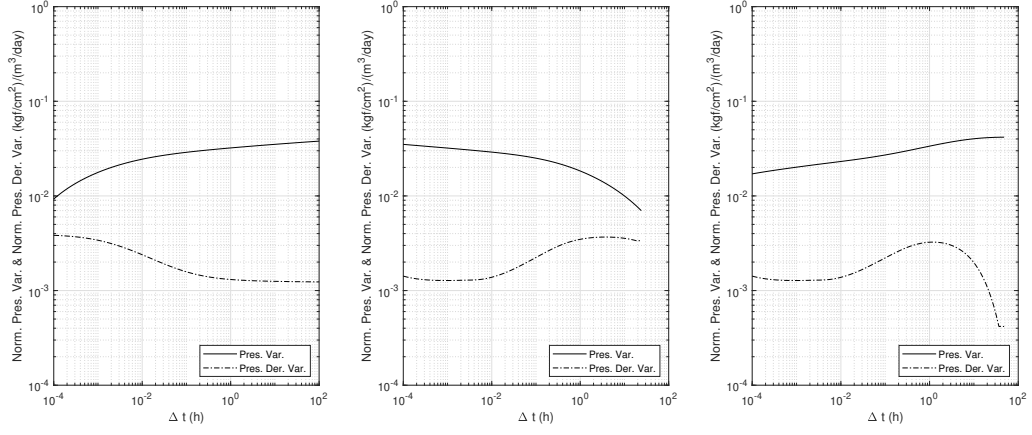


(b) 4th, 5th and 6th injection period

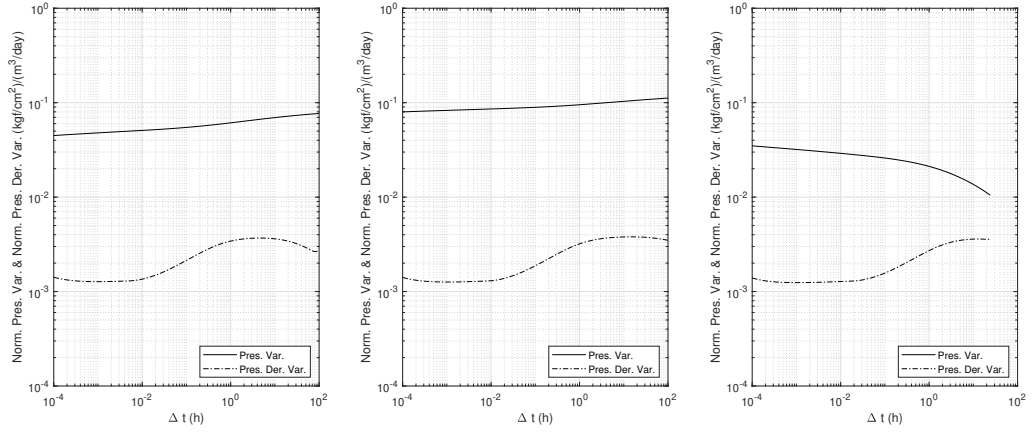
Figure 8: Normalized pressure and pressure derivative curves for case C2

Cases	Layers	$k_j$ (mD)	$h_j$ (m)	$\mu_o$ (cP)	$\hat{M}$	$\phi$
A1	3	1000	10	5.0	3.20	0.2
A2		500	15	1.0	0.64	
		100	20			
B1	3	1000	10	5.0	3.20	0.2
B2		500	15	1.0	0.64	
		100	20			

Table 2: Rock and fluid properties for cases A and B



(a) 1st, 2nd and 3rd injection period

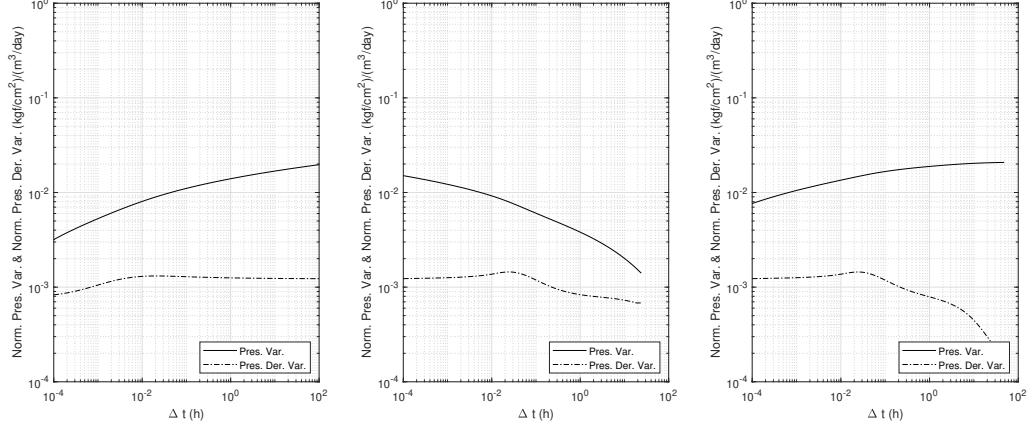


(b) 4th, 5th and 6th injection period

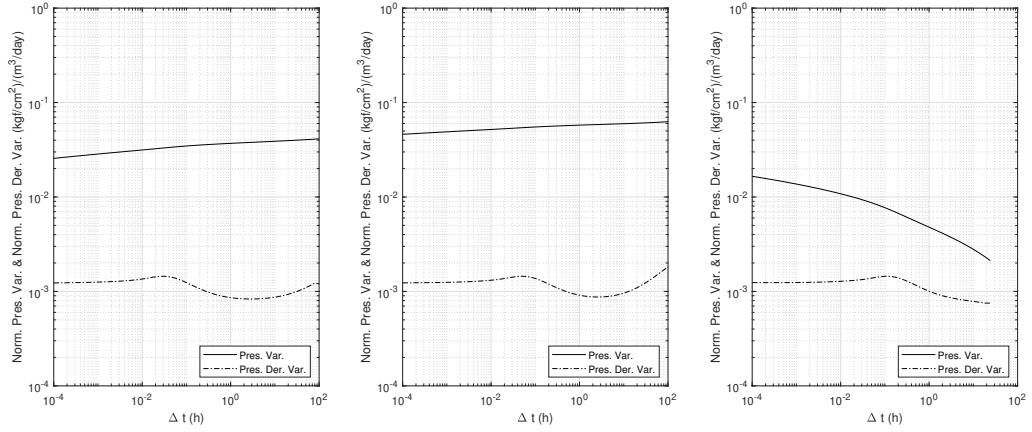
Figure 9: Normalized pressure and pressure derivative curves for case D1

Case	Injection time (h)	Flow-rate scheme ( $m^3/day$ )
C and D	120	1000
	24	0
	48	500
	100	1000
	200	1500
	24	0

Table 3: Flow-rate schemes for cases C and D



(a) 1st, 2nd and 3rd injection period



(b) 4th, 5th and 6th injection period

Figure 10: Normalized pressure and pressure derivative curves for case D2

Cases	Layers	$k_j$ (mD)	$h_j$ (m)	$\mu_o$ (cP)	$\hat{M}$	$\phi$
C1	2	1000	10	5.0	3.20	0.2
C2		500	15	1.0	0.64	
D1	3	1500	8	5.0	3.20	0.2
D2		750	10	1.0	0.64	
		250	12			

Table 4: Rock and fluid properties for cases C and D

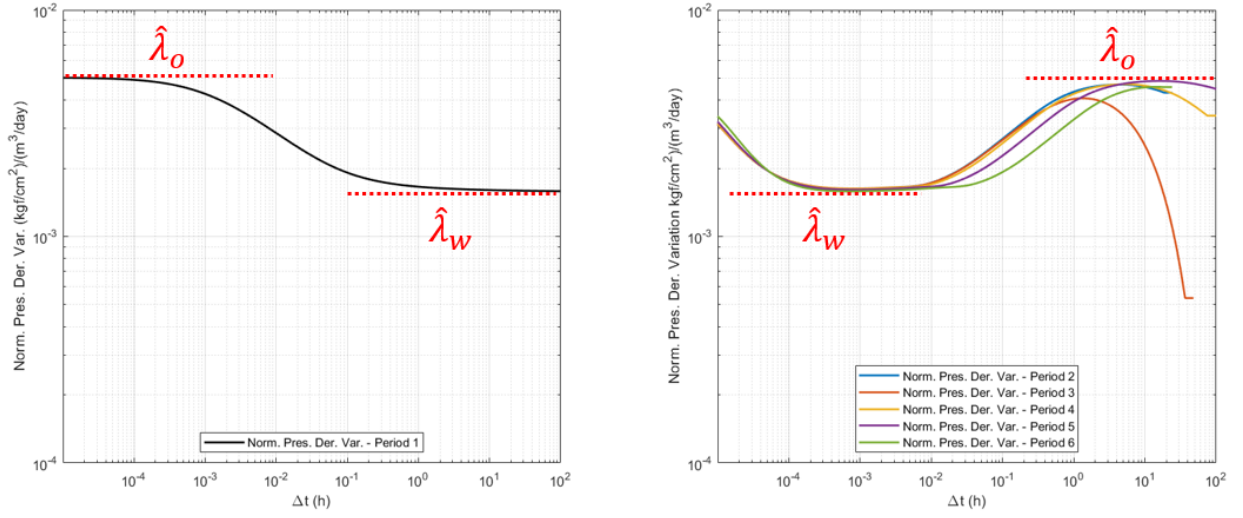


Figure 11: Normalized pressure derivative curves for case C1

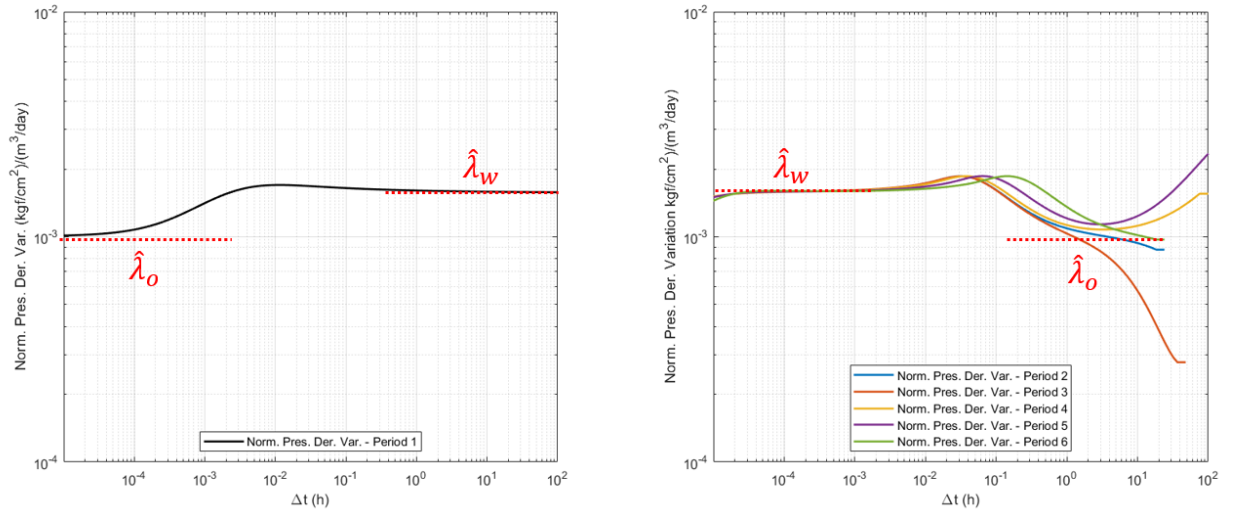


Figure 12: Normalized pressure derivative curve for case C2

Case	$k_{eq}$ (mD)	Period	$k_{eqo}$ (mD)	Error (%)	$k_{eqw}$ (mD)	Error (%)
C1	700	1	700.47	0.07	693.46	-0.93
		2	700.51	7.32	676.05	-3.42
		3	863.27	23.32	676.15	-3.41
		4	749.13	7.02	678.01	-3.14
		5	724.51	3.50	683.68	-2.33
		6	770.41	10.06	695.01	-0.71

Table 5: Estimated equivalent permeability results for case C1

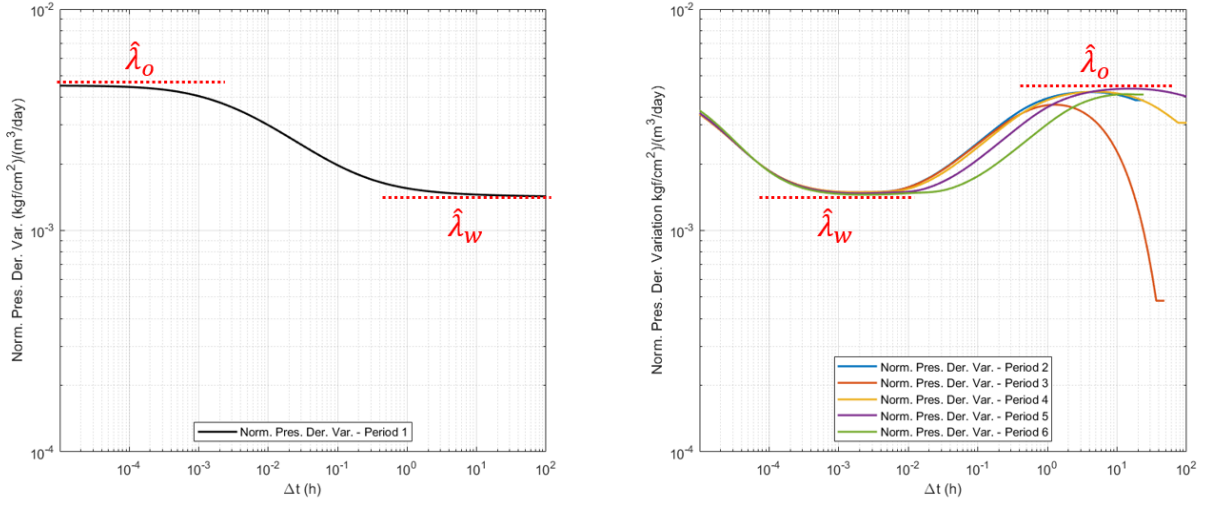


Figure 13: Normalized pressure derivative curve for case D1

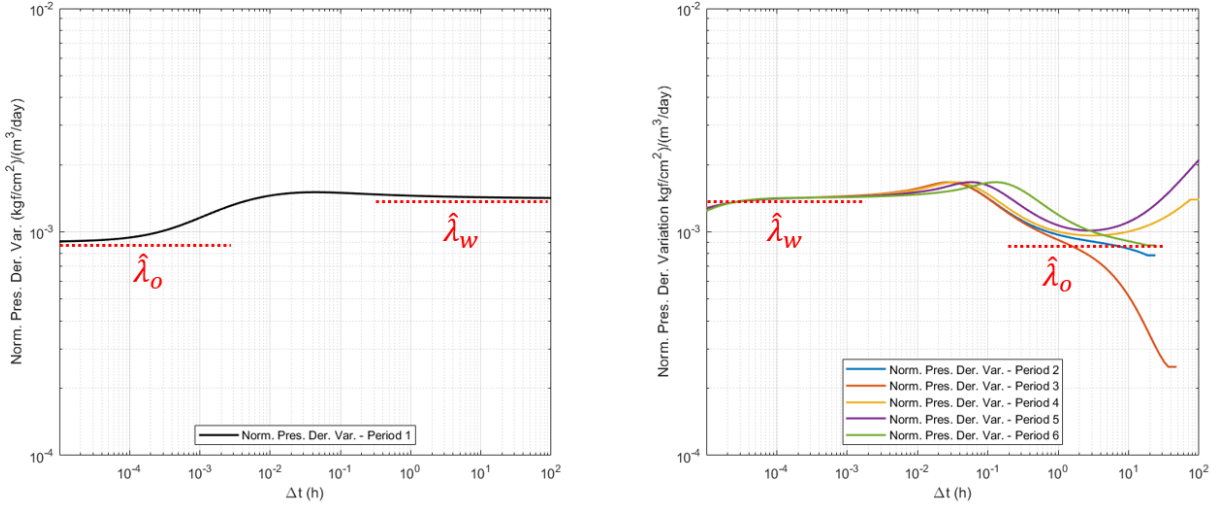


Figure 14: Normalized pressure derivative curve for case D2

Case	$k_{eq}$ (mD)	Period	$k_{eq_o}$ (mD)	Error (%)	$k_{eq_w}$ (mD)	Error (%)
C2	700	1	699.19	-0.12	696.37	-0.52
		2	702.30	0.43	701.97	0.28
		3	710.53	1.50	700.55	0.08
		4	653.47	-6.65	699.89	-0.02
		5	610.56	-11.49	698.94	-0.15
		6	706.79	0.97	696.24	-0.54

Table 6: Estimated equivalent permeability results for case C2

Case	$k_{eq}$ (mD)	Period	$k_{eqo}$ (mD)	Error (%)	$k_{eqw}$ (mD)	Error (%)
D1	750	1	749.90	-0.01	741.002	-1.20
		2	798.26	6.43	717.31	-4.36
		3	902.41	20.42	718.13	-4.25
		4	796.08	6.14	720.23	-3.97
		5	772.81	3.04	726.55	3.13
		6	815.12	8.68	735.57	1.92

Table 7: Estimated equivalent permeability results for case D1

Case	$k_{eq}$ (mD)	Period	$k_{eqo}$ (mD)	Error (%)	$k_{eqw}$ (mD)	Error (%)
D2	750	1	749.30	-0.09	745.74	-0.57
		2	752.04	0.27	744.34	-0.75
		3	773.01	3.07	748.60	-0.19
		4	705.54	-5.93	747.14	-0.48
		5	672.76	-10.40	745.73	-0.57
		6	756.30	0.84	742.78	-0.96

Table 8: Estimated equivalent permeability results for case D2